Thermal characterization of jatropha-oil blends in the 20–55°C temperature range and tribological study

G. Lara-Hernández and K. Morales Almanza

División de Estudios de Posgrado e Investigación, Instituto Tecnológico de Orizaba, Orizaba, Ver. México

F.A. Domínguez-Pacheco

Sección de Estudios de Posgrado en Investigación-ESIME-IPN, U.P.A.L.M., Col. San Pedro Zacatenco, 07730 Ciudad de México, México

A. Cruz-Orea

Centro de Investigación y de Estudios Avanzados del IPN, Av. IPN No. 2508, Col. San Pedro Zacatenco, 07360, Ciudad de México, México

H. Herrera Hernández

Centro Universitario UAEM Valle de México, Edo. de Méx., México

S. Vijay Kumar

Department of Mechanical Engineering, Nitte Meenakshi Institute of Technology, Bangalore - 560064, Karnataka, India

J. J. A. Flores-Cuautle

Secihti/Tecnológico Nacional de México/I.T. Orizaba, México 94300, México

Received 14 November 2024; accepted 23 September 2025

The increasing need for sustainable industrial supplies makes the use of vegetable oil additives a viable option for making industries more environmentally friendly. In this sense, the use of vegetable-based oils can reduce the friction coefficient of oil, decrease wear rates over working temperature ranges, and decrease environmental impact by extending equipment lifetime and potentially reducing the need for oil changes. In this work, motor oil-Jatropha blends at different ratios (97:3, 95:5, 92:8, and 90:10) were investigated for their thermal properties as a function of temperature, and a tribological characterization was performed to obtain the friction coefficients from each motor-Jatropha oil blend. Within the studied temperature range, the results indicate that it is possible to modify the thermal properties or even the friction coefficient by adjusting the mixture ratio. In this work, a further investigation on refined Jatropha as a lubricant oil additive is presented, adding the variation of thermal properties in the temperature range of $20 - 55^{\circ}$C.

Keywords: Vegetable oil; tribological characterization; multidimensional analysis.

DOI: https://doi.org/10.31349/RevMexFis.72.020601

1. Introduction

The mitigation of environmental problems has increased the need for ecologically friendly resources such as agriculture [1, 2], fiber composites [3, 4], and especially those related to transportation [5, 6]. Because the primary source of contamination in transportation is fuel, several attempts have been made to obtain green fuels. Jatropha curcas oil has been used as a biofuel and as an additive in lubricant oils [7–9]; therefore, knowledge of its thermal properties and tribological behavior is needed.

On the other hand, some other applications in which oil's thermal properties are critical can be mentioned like thermal baths in biomedical and laboratory incubators that make use of oils instead of water to maintain the temperature stable for sensitive experiments [10], in electric-powered vehicles, lithium-ion batteries have started being cooled using oils, therefore, it is necessary to research the modifications in the thermal properties of these oils [11].

Lubricants are fossil-origin products with rust and wear protection as primary targets. This primary objective involves obtaining information about the mechanical properties of the lubricant to match the desired application.

Oil production can be classified according to the oil source, *i.e.*, mineral, animal, or vegetable, and vegetable oils can further be divided into edible and non-edible plants. Among the non-edible plant oil producers, Jatropha curcas (Jatropha), Pongamina pinnata (Karanja), Madhua indica, Calophyllum inophyllum (Polanga), and Hevea brasiliensis (Goma) can be mentioned [12–15]. Jatropha is the most studied plant, and it is used in biodiesel production, providing economic, sociological, and environmental advantages [16, 17].

TABLE I. Composition of several varieties of Jatropha oil.

Fatty acid	Content (%)
Palmitic	13.18 -17.84
Palmitoleic	0.33 - 0.55
Stearic	6.48 -12.75
Oleic	30.39 - 42.66
Linoleic	31.41 - 44.67

Jatropha is a bush that is five meters tall at a maximum and has developed in different climates and soils, in addition to having a long life, short growth time, and constant fruit production. The Jatropha fruits are non-edible and have a high oleic acid content, making this bush a profitable and easy-to-harvest product. The specific fatty acid content depends on several factors, including variety, harvest region, and amount of water (see Table I) [18–20]. Although several parts of Jatropha can be used, most studies are related to seeds, mainly to size and oil-obtaining methods. Jatropha is one of the most promising alternatives to conventional diesel fuel because of its high content of fatty acids and triglycerides [18–20]. It is also used as a raw oil source; therefore, its behavior as a lubricant additive is worth researching.

The thermal and tribological properties stand out among the properties of interest for industrial applications. The most prominent parameters are the thermal effusivity (e), thermal diffusivity (α), thermal conductivity (κ), density (ρ), specific heat capacity (C_p), wear print (W), and friction coefficient (μ).

Jatropha can reduce wear, lower the friction coefficient, and improve thermal properties when used as an additive in motor oil at 95:5 and 90:10 motor/Jatropha ratios [7–9]. Thermal properties are related to tribological properties; therefore, it is reasonable to complement the thermal properties of such mixtures at intermediate ratios of 97:3 and 92:8. Motor oil/Jatropha mixtures were studied at temperatures ranging from $20 - 55°$C to obtain further information.

2. Materials and methods

The mixtures were made with SAE 15W40 commercial oil as the mixture base oil because of its mineral origin and working temperature (from now on SAE, Quartz®,5000M), and refined Jatropha oil (RJ) was used as the additive (Centro de Desarrollo de Productos Bióticos, Mex.). The thermal properties of this particular SAE oil are widely available in the literature [8, 21].

Jatropha Curcas L. is from the Euphorbiaceae family, and this variety was selected because it has oily seeds; at the same time, it provides a new application for non-edible seeds. The refined Jatropha shows a density of $\rho = 868.55$ Kg/m^3, and $40 - 55$ cP for viscosity at room temperature (RT$= 22°$C) whereas the selected motor oil $\rho = 896$ Kg/m^3 [8, 22].

The reported thermal properties of refined Jatropha and unrefined Jatropha are similar at RT (thermal effusivity 5.25 and 5.21×10^2 Ws$^{1/2}$/m^{2}K, thermal diffusivity of 10 and 9.22×10^{-8} m^2/s, thermal conductivity of 1.65 and 1.59×10^{-1} W/mK respectively) [8]. When the Jatropha oil is used as a lubricant, unrefined Jatropha presents bigger wear scars compared to the RJ oil; thus, the refined Jatropha oil was used in this work.

The studied mixtures were prepared as follows: the motor oil was added to a sterile container via pipettes (10 ± 0.04 ml, PYREX), and the vegetal oil was added via a micro-pipette (20 ± 0.2 μl, Eppendorf). The mass of the mixture was determined using a precision balance (OHAUS DV214C, 0.1 mg). The oils were mixed using an electronic stirrer (Wigger Hauser, HPS 630). Mixtures were made at room temperature, at 1100 rpm for 30 minutes before each measurement.

2.1. Thermal techniques

The lubricant properties of oils depend on their thermal properties as stated by the Prandtl number, which can be represented as the relationship between kinetic viscosity (also known as momentum viscosity or viscous diffusivity) and thermal diffusivity $Pr = v/\alpha$ [23]; thus, research on the thermal properties of oil mixtures as a function of temperature is highly recommended.

2.1.1. Calorimetry

The specific heat capacity indicates the amount of heat required to raise the sample temperature by $1°$K. It can be calculated from the thermal effusivity, thermal diffusivity, and density ($C_p = e\rho^{-1}\alpha^{-1/2}$), or it can be measured directly. Adiabatic scanning calorimetry (ASC) is used to measure the specific heat capacity. This technique is based on applying a constant heat over a sample and then obtaining the specific heat capacity from the enthalpy change in an isobaric environment ($dH = dQ$):

$$C_p = T\frac{dS}{dT} = \frac{dQ}{dt}\frac{dt}{dT} = P\left(\dot{T}\right)^{-1},$$

where C_p is the specific heat capacity (dQ/dT), T is the temperature, S is the entropy (dQ/T), Q is the supplied heat, t is the time, P is the power supplied (dQ/dt), and $\dot{T}$ is the temperature scanning rate (dT/dt) [24].

The employed ASC is formed by a sample cell placed in an adiabatic environment; the adiabatic environment uses two thermal shields. Because the heat exchange between the sample and the surroundings directly impacts the measurement precision, the calorimeter employs a vacuum in the 10^{-4} mbar to further reduce the sample heat loss due to convection [25]. The temperature of the sample cell and the first shield is controlled in such a way that the temperature between them is zero. The second shield is placed in a thermal bath at a constant temperature. The temperatures of the

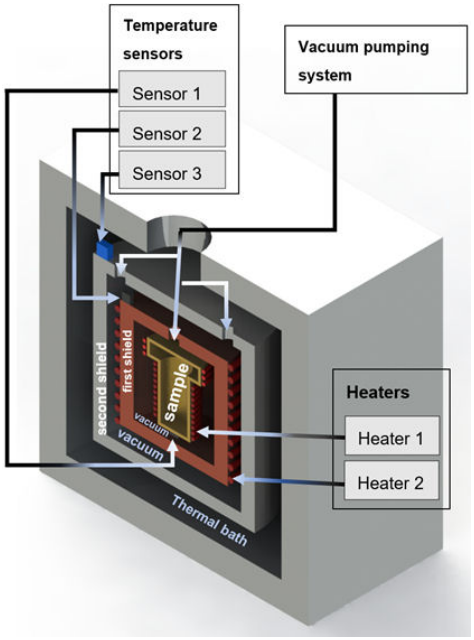

FIGURE 1. Adiabatic scanning calorimeter.

sample cell and shields are monitored, as shown in Fig. 1. The procedure to carry out calorimetry measurements is as follows: 12 ml of sample in place in the sample container. The amount of the sample is due to the sample container capacity. The sample is placed in the container at RT. Since the thermal bath employs water and no chill system was used, measurements were made in the 30° to 90°C temperature range.

2.1.2. *Thermal effusivity and diffusivity*

The frontal photopyroelectric technique (also known as an inverse photopyroelectric technique) was used for thermal effusivity and diffusivity measurements. In this technique, a frequency-modulated laser (f) is directed to one side of a pyroelectric sensor, with the sample positioned on the opposite side. A frequency sweep is then performed. The pyroelectric material is from the Lead Zirconate Titanate (PZT) family, 500 μm thick, and has well-known thermal properties. Detailed experimental setups can be found in the literature [21, 26]. The pyroelectric signal is a function of the thermal properties of the sample, the thermal properties of the pyroelectric, and the light modulation frequency. The frequency range was chosen to obtain thermal effusivity and thermal diffusivity at the same time; then, it is possible to obtain thermal conductivity by using a mathematical relationship.

The frequency range spans from 0.1 to 10 Hz, making the pyroelectric thermally thin at the lowest frequencies and thermally thick at the highest frequencies. Therefore, the frequency at which the pyroelectric changes from thermally thin to thermally thick is in the middle of the frequency range.

Thermal effusivity can be obtained using the thermally thick pyroelectric, expressed as the product of the pyroelectric thermal diffusivity times its thickness, which should be greater than one, $a_p L_p > 1$. The product $a_p L_p$ is defined by $L_p\sqrt{\pi f/\alpha_p}$, where L_p and α_p refer to the pyroelectric thickness and thermal diffusivity, respectively.

Then, for a thermally thick sample, the pyroelectric signal is normalized using Eq. (1).

$$V_N(f) = \frac{V_s(f)}{V_g(f)}. \tag{1}$$

With $V_s(f)$, the pyroelectric signal with the sample under research is placed on the opposite side of the pyroelectric sensor, and $V_g(f)$, the pyroelectric signal when the opposite side of the pyroelectric sensor is air. This is made to compensate for thermal parameters that depend only on the pyroelectric sensor, thus making the thermal parameters of the pyroelectric sensor constant.

$$V_s(f) = \frac{\left(1-e^{(1+j)a_pL_p}\right)\left(1+\frac{e_s}{e_p}\right)+\left(e^{-(1+j)a_pL_p}-1\right)\left(1-\frac{e_s}{e_p}\right)}{e^{-(1+j)a_pL_p}\left(\frac{e_g}{e_p}-1\right)\left(1-\frac{e_s}{e_p}\right)+e^{(1+j)a_pL_p}\left(1+\frac{e_g}{e_p}\right)\left(1+\frac{e_s}{e_p}\right)}) \,. \tag{2}$$

With $j^2 = -1$, e_i is the thermal effusivity, and the subindex $i = p, g, s$ refers to the pyroelectric, air, and sample, respectively.

$$V_g(f) = \frac{\left(1-e^{(1+j)a_pL_p}\right)\left(1+\frac{e_g}{e_p}\right)+\left(e^{-(1+j)a_pL_p}-1\right)\left(1-\frac{e_g}{e_p}\right)}{e^{-(1+j)a_pL_p}\left(\frac{e_g}{e_p}-1\right)\left(1-\frac{e_g}{e_p}\right)+e^{(1+j)a_pL_p}\left(1+\frac{e_g}{e_p}\right)^2}) \,. \tag{3}$$

The normalized signal as a function of the frequency depends on the sensor and sample thermal effusivity; thus, it is possible to obtain the sample thermal effusivity by knowing the sensor's thermal effusivity. Thermal diffusivity can be obtained by using the relationship between the phases of a reference sample and the sample under analysis. When the pyroelectric is thermally thin ($a_pL_p \ll 1$), the thermal diffusivity can be obtained using the tangent of the phases' ratio [27].

$$\alpha_s = \alpha_w \left(\frac{\tan\phi_s}{\tan\phi_w}\right). \tag{4}$$

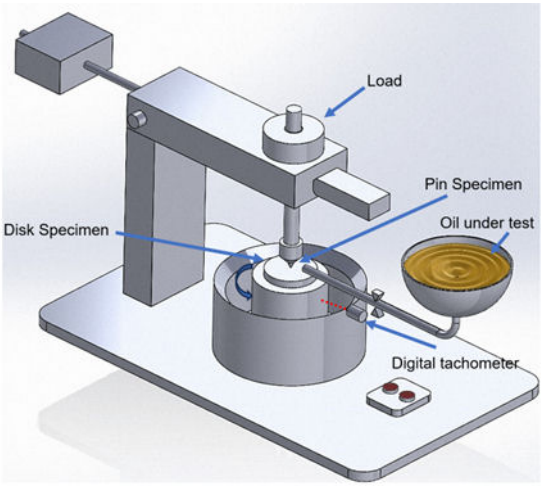

FIGURE 2. Experimental setup used to obtain the frictional coefficient by the Pin on Disk method.

The thermal conductivity of the sample (k_s) can be calculated from the thermal relationship between the thermal effusivity and thermal diffusivity of the sample ($k_s = e_s\sqrt{\alpha_s}$); thus, a complete thermal characterization is obtained.

2.1.3. *Density*

Density was determined using the volume and the mass; the oil mixture was placed in a graduated cylinder and sealed to ensure a constant mass, and a thermometer was used to get the mixture temperature. The mixture was placed in a silicone oil bath to reduce the influence of temperature changes. When the sample density, thermal diffusivity, and thermal effusivity are known, the mass-specific heat can be calculated using the relationship $c_p = e_s/\rho\sqrt{\alpha_s}$.

2.1.4. *Tribological measurements*

The pin-on-disk method consists of a metal pin pressed, at controlled force, over a rotating disk; when the lubricant is the analyzed sample, the pin and the disk are made of materials with known mechanical properties like hardness, and the friction coefficient is measured as a time function as shown in Fig. 2. The wear test was performed using an axial load of 4.905 N and 0.66 m/s velocity during 300 s. Chromed steel spheres, 1 cm in diameter, and 5 cm in diameter carbon steel 1018 plates, 1.26 cm thick, were used for wear studies to test the oil mixtures' lubricant capability.

3. Results and discussions

The mixture densities are shown in Fig. 3 as a temperature function; the 100% motor and Jatropha densities are also shown for comparison purposes. It can be seen that 97:3, 95:5, and 92:8 mixture ratios have similar values over the entire temperature range, whereas the 90:10 mixture ratio presents the lowest density. Because Motor and Jatropha oils

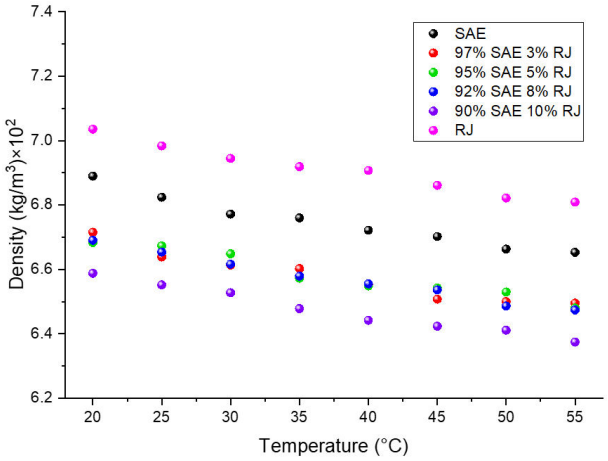

FIGURE 3. Density of samples as a function of temperature.

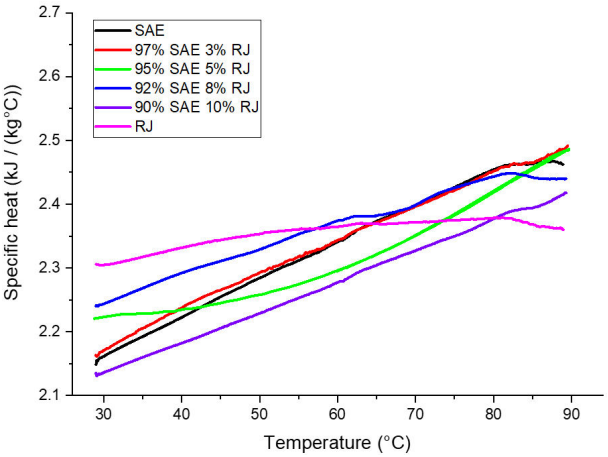

FIGURE 4. Specific heat (C_p) of samples as a function of temperature.

show a similar trend, the mixtures are expected to behave similarly.

As mentioned in the methodology section, thermal conductivity and specific heat can be calculated from thermal effusivity, thermal diffusivity, and density. Calculating thermal conductivity and specific heat using the thermal relationship involves error propagation; therefore, as a way to have another source of information, the specific heat was measured using a calorimeter, thereby obtaining the samples' behavior as a function of temperature.

Specific heat is presented in Fig. 4, and it should be noted that Jatropha's specific heat behaves differently from the rest of the analyzed samples. For instance, the slope of a linear fitting of Jatropha's specific heat is 1.02×10^{-2}, whereas the slope of linear fittings from the rest of the samples is within the range 3.54×10^{-2} to 5.28×10^{-2}. The 90:10 sample exhibits the most stable growth rate behavior as a function of temperature.

Figure 5 shows the thermal effusivity for the studied samples. The inset in Fig. 5 shows an example of the pyroelectric signal for a selected sample. The thermal effusivity calcula-

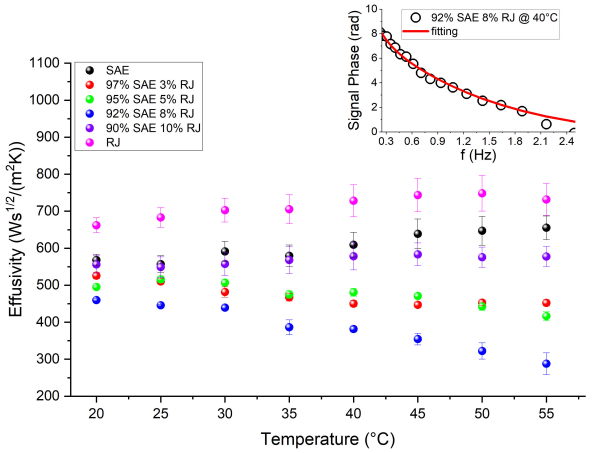

FIGURE 5. Thermal effusivity of the samples as a temperature function. Inset: An example of the pyroelectric signal for a selected sample, open circles are the experimental points, and the solid line is the best fit of Eq. (2) to the experimental data.

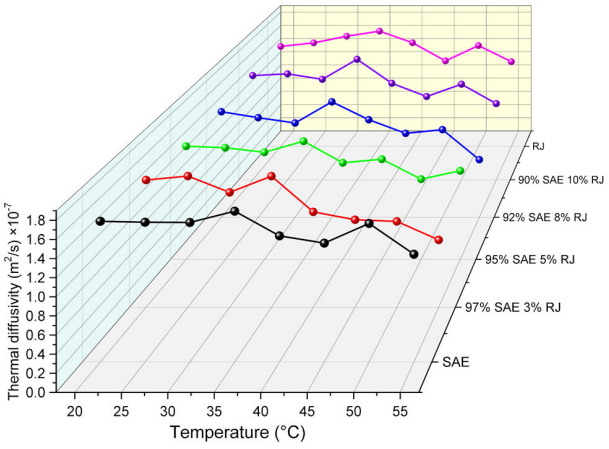

FIGURE 6. Thermal diffusivity of the studied samples in the $20 - 55°$C range.

tion involves fitting Eq. (1) to the experimental points; therefore, a fitting error appears. The error bar presented in Fig. 5 accounts for the error in the calculation of thermal effusivity due to the fitting procedure. It should be noted that all samples' behavior can be approximated by a linear function, with RJ and 90:10 having the slope closest to zero within the analyzed temperature range.

The thermal diffusivity for the studied oils is shown in Fig. 6, diffusivity values were calculated using Eq. (4).

3.1. Friction coefficient as a time function

The wear test gives the friction coefficient as a time function for the studied samples; the results for the studied ratios are shown in Fig. 7, and the non-lubricated sample is also shown for comparison purposes. The friction coefficients are in the ranges of 5-8.5, 0.29-0.34, 0.22-0.26, 0.16-0.26, 0.20-0.24, 0.23-0.28, 0.15-0.17 for the motor-Jatropha oil combinations

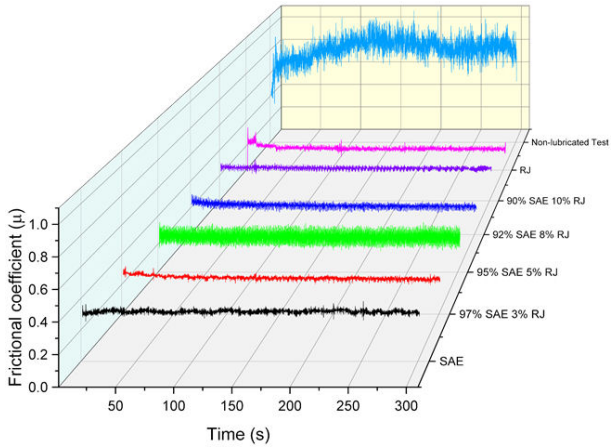

FIGURE 7. Frictional Coefficient of motor Oil (SAE), Jatropha oil (RJ), and studied mixtures, obtained by the Pin on Disk method.

TABLE II. Average values of friction coefficient (μ) of SAE, RJ, and studied mixtures.

Oil	$\mu(\times 10^{-1})$	$\sigma(\times 10^{-2})$
SAE	3.15	1.54
97% SAE 3% RJ	2.46	1.81
95% SAE 5% RJ	2.51	4.65
92% SAE 8% RJ	2.20	1.88
90% SAE 10% RJ	2.58	1.29
RJ	1.83	1.86

of non-lubricated, SAE 100%, 97:3, 95:5, 92:8, 90:10, and RJ 100%, respectively.

Table II shows that the SAE 92%-RJ8% ratio presents the lowest friction coefficient as a time function compared to other SAE/RJ combinations. On the other hand, RJ oil displays the lowest friction coefficient compared to the studied samples.

3.2. Discussion

As already pointed out for Contreras and Gallardo, the refined Jatropha mixtures present the most significant changes in their thermal properties within the 0 to 10% Jatropha content [7, 8]; therefore, this work fills the gap about the thermal properties for mixtures in the range where the significant changes in thermal properties take place.

The refined Jatropha has the smallest specific heat slope, indicating thermal stability; at the same time, it has the smallest friction coefficient. As a drawback, the price of using pure RJ can be expensive for some applications; therefore, when thermal stability is the goal, RJ is the option of choice, but at a cost. The SAE 97:3 has a similar specific trend as the temperature function of motor oil and a friction coefficient between the SAE and RJ. On the other hand, despite the SAE 95:5 combination presenting a similar friction coefficient to the rest of the combinations, a higher standard deviation in the friction coefficient was observed.

Thermal effusivity can be modified with a linear-like trend as a temperature function, and thermal effusivity varies over a range between 300 and 700 $Ws^{1/2}/m^2K$, which spans an opportunity for tuning thermal properties for specific applications.

4. Conclusion

Combining Jatropha with motor oil enhances the lubricant properties, thus lowering friction. The 97:3 and 92:8 combinations give reduced friction coefficients compared to pure motor or Jatropha oils. Pure refined Jatropha exhibits better lubricating properties in friction coefficient measurements, but at a cost. For this reason, the 92:8 blend appears as the better option to reduce friction. Density diminishes with temperature as the theory indicates, with the same trend for all blends.

It is worth mentioning that the temperature of the tested oils changes during tribological measurements. The generated friction is released as heat in the tested oil. In this work, the oil temperature was not monitored during the test; this limitation should be taken into account in future studies.

1. R. Kumar *et al*., Earthworms for Eco-friendly Resource Efficient Agriculture, In Resources Use Efficiency in Agriculture, pp. 47-84 (Springer Singapore, 2020), https://doi.org/10.1007/978-981-15-6953-1_2
2. A. Sahoo *et al*., Utilization of fruit and vegetable waste as an alternative feed resource for sustainable and eco-friendly sheep farming, *Waste Management* **128** (2021) 232, https://doi.org/10.1016/j.wasman.2021.04.050
3. H. Abdellaoui *et al*., Mechanical behavior of carbon/ natural fiber-based hybrid composites, In Mechanical and Physical Testing of Biocomposites, Fibre-Reinforced Composites and Hybrid Composites, pp. 103-122 (Elsevier, 2019), https://doi.org/10.1016/b978-0-08-102292-4
4. N. Hossain *et al*., Synthesis and Characterization of Eco-Friendly Bio-Composite from Fenugreek as a Natural Resource, *Polymers* **14** (2022) 5141, https://doi.org/10.3390/polym14235141.
5. O. Edenhofer *et al*., Mitigation of climate change: Contribution of working group III to the fifth assessment report of the intergovernmental panel on climate change, *Cambridge University Press* **1454** (2014) 147.
6. E. N. Trikoz, D. M. Osina, and V. M. Malinovskaya, Legal aspects of encouraging and enforcing eco-friendly behavior in the transport sector, *IOP Conference Series: Materials Science and Engineering* **918** (2020) 012249, https://doi.org/10.1088/1757-899x/918/1/012249
7. E. Contreras-Gallegos *et al*., Study of Mineral-Based oils with Jatropha curcas L. as Bio-Additive Through Thermal and Kinematic Viscosity Properties, *International Journal of Thermophysics* **43** (2021), https://doi.org/10.1007/s10765-021-02932-8
8. E. A. Gallardo-Hernández *et al*., Thermal and Tribological Properties of Jatropha Oil as Additive in Commercial Oil, *International Journal of Thermophysics* **38** (2017), https://doi.org/10.1007/s10765-017-2185-y
9. F. Nieto Camacho, Comportamiento Tribologico del Aceite de Jatropha Curcas como Aditivo, Master's thesis, ESIME-IPN, CDMX, Mexico (2014).
10. E. Mestres *et al*., Characterization and comparison of commercial oils used for human embryo culture, *Human Reproduction* **37** (2021) 212-225, https://doi.org/10.1093/humrep/deab245
11. W. Cheng *et al*., Investigation of the thermal performance and heat transfer characteristics of the lithium-ion battery module based on an oil-immersed cooling structure, *Journal of Energy Storage* **79** (2024) 110184, https://doi.org/10.1016/j.est.2023.110184
12. P. K. Halder, N. Paul, and M. R. A. Beg, Prospect ofPongamia pinnata(Karanja) in Bangladesh: A Sustainable Source of Liquid Fuel, *Journal of Renewable Energy* **2014** (2014) 1, https://doi.org/10.1155/2014/647324
13. H. Ong *et al*., Comparison of palm oil, Jatropha curcas and Calophyllum inophyllum for biodiesel: a review, *Renewable and Sustainable Energy Reviews* **15** (2011) 3501, https://doi.org/10.1016/j.rser.2011.05.005
14. S. Pinzi *et al*., The Ideal Vegetable Oil-based Biodiesel Composition: A Review of Social, Economical and Technical Implications, *Energy & Fuels* **23** (2009) 2325, https://doi.org/10.1021/ef801098a
15. Vismaya *et al*., Extraction and recovery of karanjin: A value addition to karanja (Pongamia pinnata) seed oil, *Industrial Crops and Products* **32** (2010) 118, https://doi.org/10.1016/j.indcrop.2010.03.011
16. G. A. Ewunie *et al*., Factors affecting the potential of Jatropha curcas for sustainable biodiesel production: A critical review, *Renewable and Sustainable Energy Reviews* **137** (2021) 110500, https://doi.org/10.1016/j.rser.2020.110500
17. J. C. Juan *et al*., Biodiesel production from jatropha oil by catalytic and non-catalytic approaches: An overview, *Bioresource Technology* **102** (2011) 452, https://doi.org/10.1016/j.biortech.2010.09.093
18. J.-h. Guo *et al*., Catalytic conversion of Jatropha oil to alkanes under mild conditions with a Ru/La(OH)3 catalyst, *Green Chemistry* **17** (2015) 2888, https://doi.org/10.1039/c4gc02406k
19. M. Hao *et al*., Global marginal land availability of Jatropha curcas L.-based biodiesel development, *Journal of Cleaner Production* **364** (2022) 132655, https://doi.org/10.1016/j.jclepro.2022 132655
20. T. T. H. Institute, Presión arterial alta (hipertensión arterial), https:// www.texasheart.org/heart-health/ heart-information-center/topics/ presion-arterial-alta-hipertension-arterial/.

21. J. J. A. Flores Cuautle *et al*., Effect of Sunflower, Almond, and Rapeseed Oils as Additives on Thermal Properties of a Machinery Oil, *Applied Sciences* **11** (2021) 7441, https://doi.org/10.3390/app11167441

22. S. Wang *et al*., The study on the influence of oxidation degree and temperature on the viscosity of biodiesel, *Green Processing and Synthesis* **9** (2019) 182, https://doi.org/10.1515/gps-2020-0019

23. J. J. A. Flores Cuautle, Thermal properties of vegetable oils used in lubricants, *Discover Chemical Engineering* **5** (2025) 17, https://doi.org/10.1007/s43938-025-00093-w

24. J. Thoen, G. Cordoyiannis, and C. Glorieux, Adiabatic scanning calorimetry investigation of the melting and order- disorder phase transitions in the linear alkanes heptadecane and nonadecane and some of their binary mixtures, *The Journal of Chemical Thermodynamics* **163** (2021) 106596, https://doi.org/10.1016/j.jct.2021.106596

25. P. Losada-Pérez *et al*., Measurements of Heat Capacity and Enthalpy of Phase Change Materials by Adiabatic Scanning Calorimetry, *International Journal of Thermophysics* **32** (2011) 913-924, https://doi.org/10.1007/s10765-011-0984-0

26. G. Lara Hernandez *et al*., Glucose in aqueous solution thermal characterization by photopyroelectric techniques, *Rev. Mex. Fis.* **63** (2017) 4.

27. N. Morioka, A. Yarai, and T. N. Takuji Nakanishi, Thermal Diffusivity Measurement of Liquid Samples by Inverse Photopyroelectric Detection, *Japanese Journal of Applied Physics* **34** (1995) 2579, https://doi.org/10.1143/jjap.34.2579